



Active site-adjacent phosphorylation at Tyr-397 by c-Abl kinase inactivates caspase-9

Received for publication, August 14, 2017, and in revised form, October 11, 2017. Published, Papers in Press, October 24, 2017, DOI 10.1074/jbc.M117.811976

Banyuhay P. Serrano^{#1}, Hannah S. Szydlo^S, Dominique Alfandari^S, and Jeanne A. Hardy^{#2}

From the Departments of [#]Chemistry and ^SVeterinary and Animal Sciences, University of Massachusetts, Amherst, Massachusetts 01003

Edited by George N. DeMartino

Caspase-9 (casp-9) is an initiator caspase and plays a central role in activating apoptotic cell death. Control of all caspases is tightly regulated by a series of phosphorylation events enacted by several different kinases. Caspase-9 is the most heavily phosphorylated of all caspases, with phosphorylation of at least 11 distinct residues in all three caspase-9 domains by nine kinases. Caspase-9 phosphorylation by the non-receptor tyrosine kinase c-Abl at Tyr-153 reportedly leads to caspase-9 activation. All other phosphorylation events on caspases have been shown to block proteolytic function by a number of mechanisms, so we sought to unravel the molecular mechanism of the putative caspase-9 activation by phosphorylation. Surprisingly, we observed no evidence for Tyr-153 phosphorylation of caspase-9 *in vitro* or in cells, suggesting that Tyr-153 is not phosphorylated by c-Abl. Instead, we identified a new site for c-Abl-mediated phosphorylation, Tyr-397. This residue is adjacent to the caspase-9 active site but, as a member of the second shell, not a residue that directly contacts substrate. Our results further indicate that Tyr-397 is the dominant site of c-Abl phosphorylation both *in vitro* and upon c-Abl activation in cells. Of note, phosphorylation at this site inhibits caspase-9 activity, and the bulk of the added phosphate moiety appeared to directly block substrate binding. c-Abl plays both proapoptotic and prosurvival roles, and our findings suggest that c-Abl's effects on caspase-9 activity promote the prosurvival mode.

Cells undergo constant turnover to maintain normal tissue function and homeostasis. This is achieved by a delicate and dynamic balance of cellular networks involving cell proliferation and cell death signaling pathways. Apoptosis or programmed cell death is an essential pathway that proceeds via a series of biochemical reactions that ultimately result in the controlled dismantling of cellular components without adverse

impact on neighboring cells. Tight regulation of apoptosis is fundamental to attain cellular homeostasis. Defects in regulation of apoptotic pathways have been implicated in many diseases that are in nature both proliferative, such as cancer, and degenerative, like Alzheimer's and Huntington's. As such, elements involved in apoptotic signaling are recognized as attractive drug targets for the development of therapeutics for apoptosis-related diseases.

Caspases are specialized proteases that mediate the faithful execution of apoptosis. Caspases cleave protein substrates, causing either activation or inhibition, which eventually commits the cell to death. Caspases are extremely specific toward substrates, generally preferring to cleave after an aspartate (1) or glutamate (2) or, in some cases, a phosphoserine (3). Depending on where they act in the apoptotic pathways, caspases are classified as either upstream initiators (casp-2,³ -8, and -9) or downstream executioners (casp-3, -6, and -7). Because caspase activity inherently induces apoptosis, caspases are synthesized and held as inactive zymogens (procaspases). Procaspases contain an N-terminal prodomain region and the highly homologous caspase core, consisting of a large and a small subunit joined together by an intersubunit linker. Most procaspases exist predominantly as homodimeric proteins. Upon apoptosis induction, initiator caspases are recruited to complex protein scaffolds that promote activation, whereas executioner caspases depend on initiator caspases to cleave the intersubunit linker, which consequently converts the inactive procaspase into a mature, active form. Once assembled into an active form, the highly dynamic loops that compose the active site assume a conformation that allows substrate binding and catalytic cleavage, thereby initiating a cascade of reactions that eventually lead to the cell's demise. Caspases exert such a dominant impact on apoptosis that any inopportune caspase activation is deleterious to the cell. Thus, caspase expression and activation are tightly regulated by various mechanisms at different checkpoints in the cell.

Phosphorylation is recognized to be a critical mediator of apoptosis (for reviews, see Refs. 4 and 5). Caspases form a subset of kinase substrates whose functions are directly affected by

This work was supported by National Institutes of Health Grant GM 080532 (to J. A. H.) and RO1DE016289 and R24OD021485 (to D. A.). The authors declare that they have no conflicts of interest with the contents of this article. The content is solely the responsibility of the authors and does not necessarily represent the official views of the National Institutes of Health. This article contains supplemental Figs. S1–S7.

¹ Supported in part by the UMass Chemistry-Biology Interface Training Program (National Research Service Award T32 GM 08515 from the National Institutes of Health).

² To whom correspondence should be addressed: Dept. of Chemistry, 104 LGRT, 710 North Pleasant St., University of Massachusetts Amherst, MA 01003. Tel.: 413-545-3486; Fax: 413-545-4490; E-mail: hardy@chem.umass.edu.

³ The abbreviations used are: casp, caspase; Apaf-1, apoptotic protease-activating factor 1; CARD, caspase activation and recruitment domain; CED3 and CED4, cell death protein 3 and 4, respectively; CT, constitutively two-chain; SH3-SH2, Src homology 3-Src homology 2 domain; KD, kinase domain; 3D, three-domain; TEV, tobacco etch virus; IPTG, isopropyl 1-thio- β -D-galactopyranoside; DPH, 5-(1,3-diaryl-1H-pyrazol-4-yl)hydantoin; PDB, Protein Data Bank; FL, full-length.

phosphorylation (6). The initiator casp-9, for example, appears to be extremely sensitive to phosphorylation, having the largest number of phosphorylation sites reported of any caspase (Fig. 1A; for reviews, see Refs. 6–8). This suggests that phosphorylation is a strong regulator of casp-9 function. This is perhaps because phosphorylation can impact casp-9 on multiple levels, as casp-9 achieves activation in many ways, from cleavage to dimerization to protein–protein interactions to the formation of the apoptosome. Phosphorylation sites are present in all domains of casp-9 (Fig. 1A) and are targeted by kinases that are involved in cell cycle (9, 10), cellular stress (11–13), and extracellular signals (14, 15).

In general, phosphorylation of caspases results in apoptotic suppression, which is a direct consequence of caspase inhibition. Intriguingly, of all the reported sites of phosphorylation in casp-9, Tyr-153 is the only site reported to activate casp-9 (12). All other sites of phosphorylation reportedly have led to inactivation (16). Tyr-153 in casp-9 is reported to be phosphorylated by the non-receptor tyrosine kinase c-Abl. c-Abl is activated in response to various extrinsic and intrinsic signals, which causes it to possess both pro- and anti-apoptotic roles (for a review, see Ref. 17). c-Abl generally recognizes the sequence (I/V/L)YXXP and phosphorylates a large number of functionally diverse substrates, in part due to its ability to shuttle between the cytosol and the nucleus. Interestingly, this nucleocytoplasmic shuttling of c-Abl dictates whether its activation would promote either cell death or survival. For example, oncogenic forms of c-Abl exhibit strictly cytoplasmic localization and constitutive activity, whereas nuclear c-Abl activated by cellular stress, such as DNA damage, promotes apoptosis. This pro-apoptotic function of c-Abl has been attributed to its phosphorylation of casp-9, resulting in self-processing and subsequent activation of casp-3 (12). We were intrigued by this functional effect of c-Abl on casp-9, especially because all other sites were reported to be inhibiting upon phosphorylation. For this reason, we undertook a study of the mechanism of casp-9 activation by Tyr-153 phosphorylation. During this study we identified a new site of phosphorylation.

In the last decade, a number of cell-based studies identified sites of phosphorylation in casp-9 (16). Many excellent proteome-wide studies have annotated sites of phosphorylation in casp-9 and other caspases. Given the multitude of different cellular contexts, it has naturally been impossible to perform these large-scale, proteome-wide studies under all relevant cellular conditions. Thus, although a number of sites have been identified, it is likely that many other sites of phosphorylation by particular kinases have not yet been identified. Here we report a novel site of phosphorylation in casp-9 by c-Abl. An active site-adjacent residue, Tyr-397, is phosphorylated by c-Abl both *in vitro* and intracellularly, leading to casp-9 inhibition.

Results

Caspase-9 is composed of the caspase activation and recruitment domain (CARD) and the core, which consists of the large and the small subunit. The reported phosphorylation site Tyr-153 resides in the casp-9 large subunit (Fig. 1, A and B). In the dimeric, substrate-bound structure of casp-9, the hydroxyl group of Tyr-153 forms a hydrogen bond with Asp-350 in the

L2' loop. This interaction seems to support the position of L2' as it correspondingly interacts with L2 and L4 in the other half of the dimer to form the substrate binding groove and catalytic site (Fig. 1C). Thus, it is conceivable that phosphorylation of Tyr-153 would impact casp-9 activity. Phosphorylation of caspases typically leads to inhibition (6), yet it has been reported that upon DNA damage, Tyr-153 phosphorylation by c-Abl results in self-processing and promotes casp-9 cleavage of casp-3 (12).

Phosphomimetic Y153E has impaired catalytic efficiency compared with WT casp-9

To probe for the functional consequence of Tyr-153 phosphorylation in casp-9, we generated the glutamate phosphomimetic Y153E. Following overexpression, Y153E remained in its zymogen (uncleaved) form unlike WT casp-9, which was expressed as a mature, cleaved enzyme (Fig. 1D). Casp-9 zymogen possesses basal activity and hence readily undergoes self-processing; however, the glutamate substitution blocks function. Unlike the WT zymogen, Y153E lacked the ability to self-process (Fig. 1E) and did not exhibit any LEHDase activity (Table 1) in the zymogen form. To assess whether the observed inhibition was due to its zymogen nature and to assess whether these variants are still cleavable by other caspases, full-length Y153E was cleaved by casp-3 (Fig. 1F). Even following cleavage to generate the mature form, Y153E remained inactive (Fig. 1G). In addition, casp-9 variants at this position were expressed from a constitutively two-chain (CT) construct, which allows independent translation of the CARD+Large and the small subunits. Even in its fully mature form, CT Y153E remained inactive, suggesting that the glutamate phosphomimetic inherently inhibits casp-9 activity (Fig. 1D and Table 1). This was in contrast to a prior report, in which phosphorylation at Tyr-153 was suggested to promote casp-9 self-processing and thereby activation (12). To validate that the inhibition was a direct consequence of the phosphomimetic, an aspartate substitution (Y153D) was made and showed the same inactivating effect as the glutamate phosphomimetic, whereas the conservative phenylalanine substitution mutant (Y153F) had a ~150-fold decrease in catalytic efficiency (Table 1). Both Y153D and Y153F were also uncleaved upon overexpression, suggesting impaired self-processing abilities (Fig. 1D). Similar to Y153E, casp-3 was able to cleave Y153D or Y153F to generate mature enzymes; however, they remained inactive (Fig. 1, F and G). Moreover, the CT version of Y153F had no measurable activity, and introducing a polar amide side chain of glutamine (CT Y153Q) did not rescue activity (Table 1 and Fig. 1D). Thus, the inhibition observed was probably due to the inherent sensitivity of the Tyr-153 site. These results are in line with prior observations. This region where the L2 and L2' loops interact is extremely sensitive to mutation and post-translational modification. Substitutions that break the L2–L2' interaction disrupt caspase activity (18), and phosphorylation of Ser-257, which is also in this region, also inactivates casp-6 (19). Thus, one might anticipate *a priori* that should Tyr-153 be phosphorylated, it would be inactivating. However, given the limitation that glutamate may not be as high-fidelity a phosphomimetic for phosphotyrosine as it is for phosphoserine and phospho-

Table 1**Catalytic parameters of caspase-9 variants using Ac-LEHD-AFC as substrate**

Values reported are mean \pm S.E. of three trials performed independently on three separate days.

Casp-9 variant	K_m μM	k_{cat} s^{-1}	$10^3 \times k_{\text{cat}}/K_m$ $\text{s}^{-1} \mu\text{M}^{-1}$
Casp-9 FL			
WT	430 \pm 35	1.4 \pm 0.1	3.3
Y153E	>3,000	<0.01	<0.003
Y153D	>3,000	<0.01	<0.003
Y153F	2,804 \pm 829	0.04 \pm 0.01	0.02
Y397F	338 \pm 18	0.78 \pm 0.1	2.7
Casp-9 CT			
WT	609 \pm 35	1.8 \pm 0.03	3.0
Y153E	>3,000	<0.01	<0.003
Y153F	>3,000	<0.01	<0.003
Y153Q	>3,000	<0.01	<0.003
Y397E	961 \pm 100	0.57 \pm 0.08	0.59

lanine and incubated with active c-Abl. Y153F substitution did not abolish phosphorylation, as the small subunit was still clearly labeled with ^{32}P (Fig. 3D). Tyr-397 appears to be more solvent-exposed relative to Tyr-153; hence, it is possible that the competition for Abl recognition and phosphorylation is heavily weighted toward Tyr-397. However, making Tyr-397 unphosphorylatable (Y397F) did not force phosphorylation of Tyr-153 but almost completely eliminated casp-9 phosphorylation (Fig. 3D). We also tested CARD-deleted versions of casp-9 (ΔCARD) to increase Tyr-153 accessibility, as the CARD in full-length casp-9 is attached through a highly flexible linker and could potentially block the Tyr-153 site. Even in the absence of the CARD, only phosphorylation at the small subunit was observed (Fig. 3E). To unambiguously identify the phosphorylated site, we performed LC-MS/MS on peptide fragments following Arg-C proteolysis of c-Abl-phosphorylated WT casp-9 and observed phosphate labeling at Tyr-397 with high confidence (supplemental Fig. S1, A and B). These results clearly indicate that Tyr-397 is the dominant site for phosphorylation by c-Abl *in vitro*.

Phosphorylation of Tyr-397 leads to casp-9 inhibition

This is the first report of a novel site, Tyr-397, being phosphorylated by c-Abl. As such, it is imperative to probe whether this phosphorylation imparts functional or structural perturbations to casp-9. A modest but statistically significant inhibition of casp-9 LEHDase activity was observed when WT was phosphorylated at Tyr-397. In contrast, the activity of the unphosphorylatable Y397F variant was unchanged even after treatment with c-Abl (Fig. 4, A and B). Although full inhibition was not observed under *in vitro* phosphorylation conditions, a strong correlation between the levels of phosphorylation and casp-9 inhibition was observed (Fig. 4C). In fact, phosphocapture experiments resulted in samples with enriched levels of phosphorylated casp-9 that correspondingly exhibited higher degrees of inhibition (Fig. 4D), implying that a homogeneous population of phosphorylated casp-9 would be completely inhibited.

One of the hallmarks of suppressed apoptosis emanating from casp-9 inhibition is the attenuation of the cleavage of downstream substrates casp-3 and casp-7 (20). WT casp-9 phosphorylated by c-Abl cleaved full-length casp-7 and casp-3 more slowly than unphosphorylated WT casp-9 (Fig. 5, A and E). In

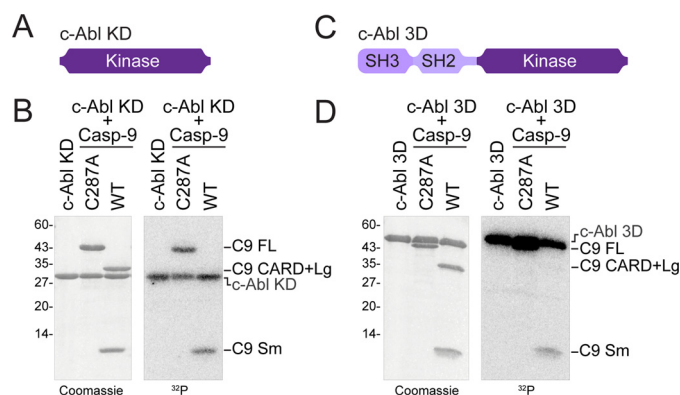


Figure 2. c-Abl phosphorylates casp-9 *in vitro* at the small subunit. A and C, recombinant c-Abl constructs used to phosphorylate casp-9 *in vitro*. The construct c-Abl KD comprises only the kinase domain, whereas the c-Abl 3D construct contains the SH3-SH2 catalytic site-inactivated variant C287A (full-length) and WT (cleaved) were subjected to *in vitro* phosphorylation by c-Abl KD or 3D in the presence of ATP + [γ - ^{32}P]ATP for 2 h. c-Abl undergoes autophosphorylation/autoactivation upon treatment with ATP. Both forms of c-Abl phosphorylated casp-9 in the zymogen (C287A) and cleaved (WT) forms. No phosphorylation in the CARD+Large region (Tyr-153 site) was detected, but phosphorylation in the small subunit was clearly visible, as shown in the autoradiograph labeled here and in the succeeding figures as ^{32}P .

contrast, there was no significant difference in the rate of casp-7 or casp-3 cleavage by casp-9 Y397F regardless of whether c-Abl was active (+ ATP) or not (− ATP) (Fig. 5, B and F). This recapitulates the previous finding that Y397F is insensitive to inactivation by c-Abl. Importantly, the degree of casp-9 phosphorylation also correlates with the decrease of its protein cleavage kinetics (Fig. 5, C and D for casp-3 and G and H for casp-7). It is worthwhile to note that Y397F is as active as WT casp-9 (Table 1); therefore, the decrease in casp-9 activity can be unambiguously attributed to phosphorylation and not simply due to inherent sensitivity of this site. Along these lines, we observed a 5-fold decrease in catalytic efficiency in the Y397E phosphomimetic (Table 1) and attenuated protein cleavage kinetics (supplemental Fig. S3, A and B). Although Y397E is not a perfect surrogate for phosphorylated Tyr-397, it manifests a functional outcome similar to Tyr-397 phosphorylation. Thus, one functional effect of Tyr-397 phosphorylation by c-Abl is to diminish casp-9's activation of executioner caspases.

Model for casp-9 inhibition by Tyr-397 phosphorylation

The substrate-binding site of active, dimeric caspases consists of highly mobile loops (L2, L3, and L4 from one monomer and L2' from the opposite monomer), which, upon substrate binding, assume a properly ordered conformation to perform catalytic cleavage. Tyr-397 is situated in loop L4 of casp-9 (Fig. 3A and supplemental Fig. S4B). In the substrate-bound structure, Tyr-397 participates in the hydrophobic network along with Ile-396 and Trp-362 to engage the hydrophobic P4 residue (supplemental Fig. S4A). Modeling a phosphotyrosine in place of Tyr-397, it appears that both the added bulk and charge of phospho-Tyr-397 would directly impact substrate binding. Being situated in a highly mobile loop, the phosphotyrosine could be envisioned to reach into the substrate-binding cavity, essentially creating steric and electrostatic

Caspase-9 phosphorylation by *c-Abl*

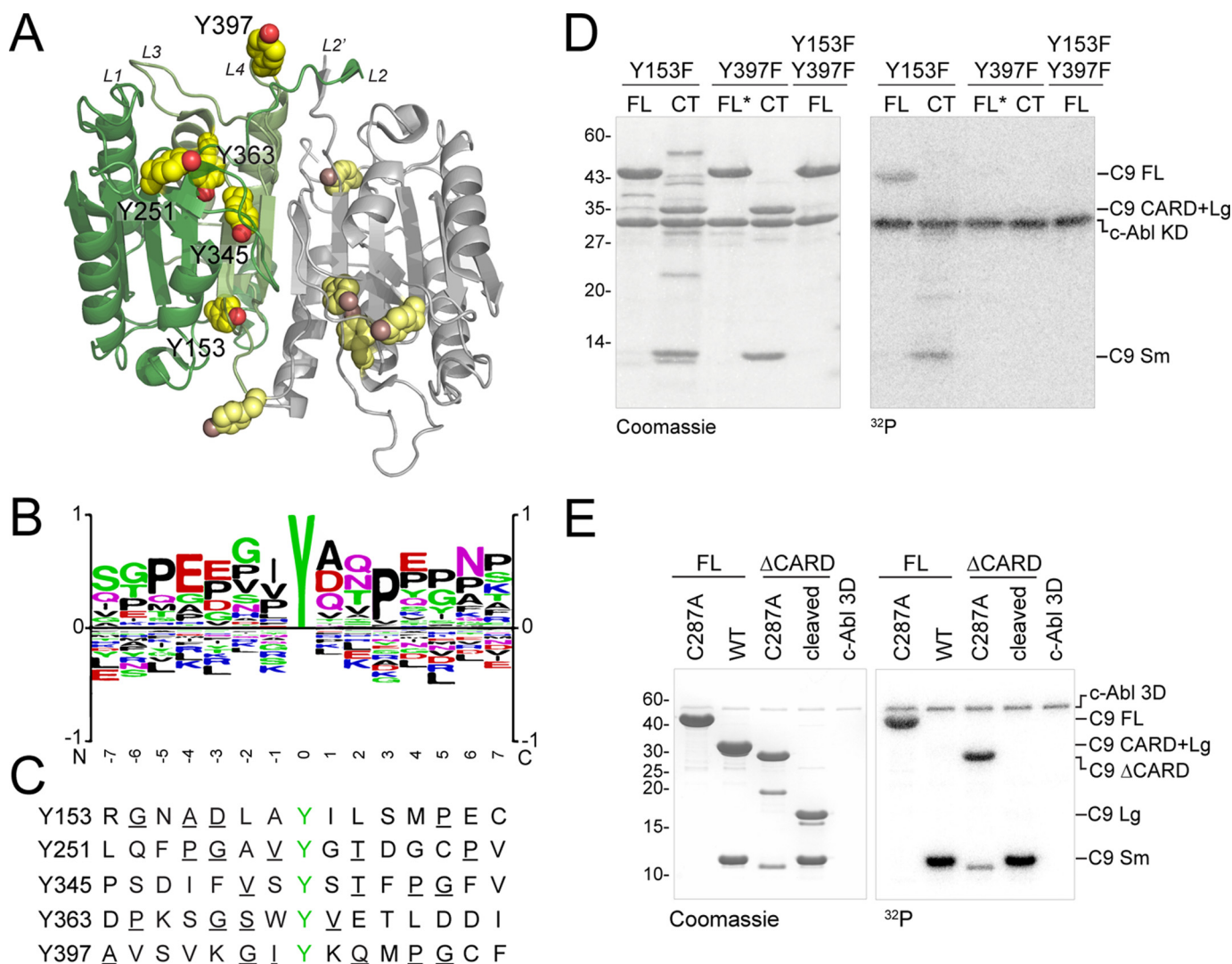


Figure 3. Tyr-397 is the predominant site for *c-Abl* phosphorylation *in vitro*. *A*, structure of casp-9 core showing all the tyrosine residues (yellow spheres). Tyr-397 (Y397) resides in loop L4 and is noticeably solvent-exposed, due to crystal contacts in this structure (PDB entry 1JXQ). *B*, substrate sequence logo for the consensus recognition sequence of *c-Abl* (downloaded from PhosphoSitePlus (33)). *C*, sequence of residues surrounding each tyrosine present in casp-9. Residues in favorable positions are *underlined*. The sequence surrounding Tyr-397 conforms well to the consensus sequence for *c-Abl* phosphorylation. *D*, unphosphorylatable casp-9 variants (phenylalanine substitutions at putative phosphorylated tyrosines) in both FL and CT versions were subjected to *in vitro* phosphorylation by *c-Abl* for 2 h. The asterisk denotes that FL Y397F was constructed in the background of C287A (catalytic cysteine-inactivated variant) to prevent self-processing because Y397F is active. FL Y153F casp-9 was still visibly phosphorylated; the CT version of Y153F revealed that the phosphorylation is in the small subunit. An absence of phosphorylation was observed for Y397F (both FL and CT) and the double mutant Y153F/Y397F. *E*, removal of the CARD in casp-9 (ΔCARD) did not promote phosphorylation of the Tyr-153 site in the large subunit. Only the small subunit was robustly phosphorylated. An unidentified nonspecific 12 kDa band from ΔCARD C287A was also observed to be phosphorylated.

clashes with other subsite residues (supplemental Fig. S4B). This would either directly obstruct the incoming substrate from binding or prevent the loop bundle from assuming an ordered conformation keeping the active site in an unproductive state, or both.

*Tyr-397 is phosphorylated in lysates and in cells upon direct *c-Abl* activation*

In vitro phosphorylation coupled with the use of unphosphorylatable protein variants has allowed identification of putative residues phosphorylated by kinases. However, alternative specificity of kinases toward substrates *in vitro* has been reported in isolated cases (21). The lack of regulatory elements normally present intracellularly has been suggested to contribute to altered phosphorylation. To determine whether Tyr-397 was a

bona fide cellular site of phosphorylation, recombinant WT casp-9 was added into HEK 293T lysates supplemented with [γ -³²P]ATP and orthovanadate, a phosphatase inhibitor. This resulted in visible phosphorylation of the CARD+Large (Fig. 6A and supplemental Fig. S5A). Given that there are other kinases readily activated by the addition of ATP and treatment of orthovanadate and that casp-9 has multiple phosphorylation sites in this region (9, 11, 13–15, 22, 23), we were not surprised by this observation. Phosphorylation of the small subunit in WT casp-9 in the absence of *c-Abl* was not evident, which could either be due to low titers of endogenous *c-Abl* in HEK 293T or because *c-Abl* was not sufficiently activated, or both. Because the activation state of *c-Abl* was not known, the lysates were supplemented with recombinant *c-Abl* to allow *in trans* activa-

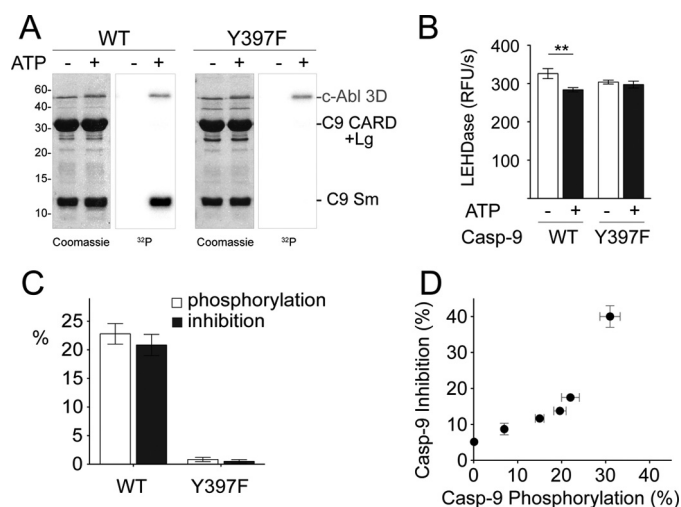


Figure 4. Phosphorylation of Tyr-397 leads to casp-9 inactivation. *A*, WT Casp-9 and the unphosphorylatable variant Y397F were subjected to *in vitro* phosphorylation by Abl in the presence or absence of ATP for 2 h. Phosphorylation of the small subunit was clearly observed in WT casp-9 but was essentially absent for casp-9 Y397F. Only background levels of phosphorylation were visible in the CARD+Large region. Gels and corresponding autoradiographs shown are representative of four independent trials performed on 4 separate days. *B*, inhibition of WT and Y397F casp-9 by phosphorylation. The activities of samples in *A* after incubation with c-Abl for 2 h were measured using the casp-9 preferred substrate *N*-acetyl-Leu-Glu-His-Asp-7-aminotrifluoromethylcoumarin. Casp-9 WT was moderately inhibited, whereas casp-9 Y397F was insensitive to c-Abl-mediated inhibition. The reduced LEHDase activity for phosphorylated WT casp-9 (+ATP) was statistically different from that of unphosphorylated WT (-ATP) (**, $p < 0.05$) as determined by Student's *t* test. Data shown are means \pm S.E. (error bars) from four independent experiments performed on 4 separate days. *C*, the level of casp-9 phosphorylation correlates with the extent of inhibition. Phosphorylation levels of casp-9 were determined from [γ - 32 P]ATP standards exposed on the same autoradiograph as the Coomassie-stained SDS-polyacrylamide gel (supplemental Fig. S2). The percentage inhibition for phosphorylated casp-9 (both c-Abl and ATP present) was normalized against activity in the non-phosphorylated form (with c-Abl but no ATP). Data shown are means \pm S.E. from four independent experiments performed on 4 separate days. *D*, correlation plot between casp-9 inhibition and casp-9 phosphorylation. WT casp-9 was initially phosphorylated *in vitro* by c-Abl and was subjected to phosphoprotein enrichment to capture a greater fraction of phosphorylated casp-9. Data shown are means \pm S.D. from three independent experiments performed on 3 separate days.

tion of c-Abl. This resulted in distinct phosphorylation of the small subunit in WT casp-9, whereas Y397F exhibited negligible levels of small subunit phosphorylation (Fig. 6A and supplemental Fig. S5, A–C). For both WT and Y397F, the CARD+Large region appeared to retain its phosphorylation state. The addition of a c-Abl inhibitor, imatinib, abrogated the phosphorylation of the small subunit but not that of the CARD+Large (Fig. 6A). This implies that the phosphorylation observed for the small subunit was predominantly due to c-Abl, whereas that for the CARD+Large was not and could be reliant on the action of other kinases.

We then proceeded to interrogate casp-9 phosphorylation in cells upon activation of endogenous c-Abl. c-Abl is known to be tightly regulated in cells, and even overexpression does not usually activate its kinase activity (24, 25); its activation is usually dependent on upstream kinases, such as Src (26), or stimulation of growth factor receptors, such as PDGFR (26). Thus, to ensure that only c-Abl is activated without activation of other kinases, HEK 293T cells were treated with 5-(1,3-diaryl-1H-pyrazol-4-yl)hydantoin (DPH), a known direct activator of c-Abl (27), as

well as the phosphatase inhibitor orthovanadate. This led to c-Abl activation, as manifested by phosphorylation of c-Abl at Tyr-412 (28). In addition, CrkII, a well-known physiological substrate of c-Abl (29), was phosphorylated only upon treatment of DPH. The presence of active, phosphorylated c-Abl and phosphorylated CrkII were confirmed by immunoblot against the phosphorylated residues pTyr-412 (for c-Abl) and pTyr-221 (for CrkII) (Fig. 6B). The c-Abl inhibitor imatinib abolished these phosphorylation events, demonstrating that c-Abl is indeed activated by DPH and vanadate (Fig. 6B). In order to probe casp-9 phosphorylation by c-Abl, HEK 293T cells were transfected with FLAG-tagged casp-9 catalytic site-inactivated variant C287A and the unphosphorylatable C287A/Y397F variant. Transfected cells were then treated with DPH/vanadate to induce c-Abl activation (Fig. 6C and supplemental Fig. S6 (A and B), panels labeled Total). Immunoprecipitated casp-9 C287A was robustly tyrosine-phosphorylated as assessed by phosphotyrosine immunoblot (Fig. 6C and supplemental Fig. S6 (A and B), panels labeled IP). Together, these data indicate that casp-9 is a *bona fide* substrate of c-Abl. Whereas phosphorylation was not entirely eliminated in the unphosphorylatable variant C287A/Y397F, the level of phosphorylation was significantly weaker than in C287A, although the total amount of immunoprecipitated casp-9 was the same in both transfected conditions (Fig. 6A and supplemental Fig. S6C). Moreover, transfected cells treated with DMSO showed weak tyrosine phosphorylation of both C287A and C287A/Y397F, the phosphorylation levels of which are comparable with that of C287A/Y397F in DPH/vanadate-treated cells (supplemental Fig. S6A). This strongly supports the model that Tyr-397 is the predominant site for c-Abl phosphorylation upon its activation by DPH and is the dominant site of c-Abl phosphorylation in cells.

Discussion

It is clear from the data presented here that Tyr-397 is a *bona fide* site of phosphorylation intracellularly, as was predicted by *in vitro* phosphorylation studies using purified proteins. There has been some suggestion in the literature that *in vitro* phosphorylation of kinase substrates sometimes differs from cellular phosphorylation (21, 30, 31). We have not previously observed irregular phosphorylation of caspase substrates by any of the kinases we have studied (19, 32, 60). Once again in this work, we found that *in vitro* phosphorylation by c-Abl accurately reflected the intracellular phosphorylation specificity we observed. This fidelity between *in vitro* and cell-based observations is probably due to casp-9 being a direct substrate of c-Abl. Our data from multiple kinase–caspase pairs suggest that when the appropriate kinase is studied, *in vitro* and cellular phosphorylation patterns are conserved (19, 32, 60).

Whereas it is clear that Tyr-397 is a *bona fide* site of c-Abl phosphorylation of casp-9, one of the most surprising aspects of our work is the fact that the reported site on casp-9, Tyr-153, was not observed to be phosphorylated by c-Abl either using purified proteins or intracellularly and was not activated by c-Abl as reported previously. This could be for a number of reasons. First, the study that identified Tyr-153 phosphorylation as activating did not investigate the functional impact of

Caspase-9 phosphorylation by c-Abl

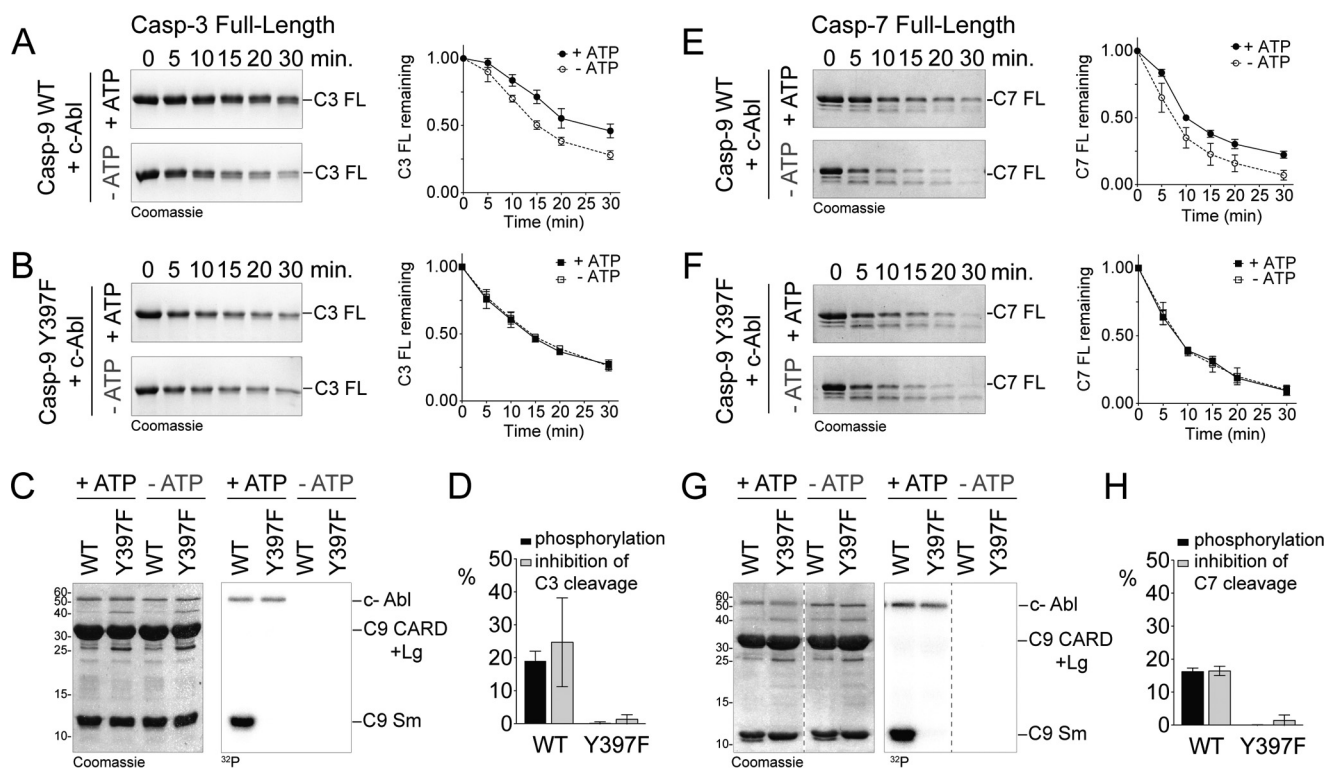


Figure 5. Phosphorylated casp-9 exhibits slower protein cleavage kinetics. WT (A) or Y397F casp-9 (B) was incubated with c-Abl in the presence or absence of ATP. 1 μ M casp-9 from the phosphorylation reaction was allowed to cleave 3 μ M full-length casp-3 C163A (catalytic site-inactivated variant) (C3 FL) for 30 min. Cleavage kinetics for each reaction are plotted as a function of the disappearance of the casp-3 FL band. C, representative Coomassie-stained gels and corresponding autoradiographs of phosphorylation reactions used in A and B. Casp-9 WT is visibly phosphorylated at Tyr-397. D, correlation between casp-9 phosphorylation as detected by autoradiography in C and inhibition of casp-3 (C3) cleavage after 30 min as shown in A and B. E and F, casp-9 WT or Y397F was incubated with c-Abl in the presence or absence of ATP. 1 μ M casp-9 from the phosphorylation reaction was allowed to cleave 3 μ M full-length casp-7 C186S (catalytic site-inactivated variant) (C7 FL) for 30 min. Cleavage kinetics for each reaction are plotted as a function of the disappearance of the casp-7 FL band. G, representative Coomassie-stained gel and corresponding autoradiograph of phosphorylation reactions used in E and F. Casp-9 WT is phosphorylated at Tyr-397. H, correlation between casp-9 phosphorylation as detected by autoradiography in G and inhibition of casp-7 (C7) cleavage after 30 min as shown in E and F. Data shown for all of the above experiments are means \pm S.E. (error bars) from three independent experiments done on 3 separate days.

substitutions at Tyr-153 on proteolytic activity but assumed that Y153F casp-9 was proteolytically active (12). In this work, we have shown that Y153F has severely reduced but detectable activity in the uncleaved form and is intrinsically inactive in the cleaved form (Table 1 and Fig. 1 (D, F, and G)). The lack of casp-9 activation led to the interpretation that Y153F-transfected cells were less susceptible to cell death due to the absence of phosphorylation by c-Abl (12), when in fact, cells should have been rendered less susceptible to cell death due to the lack of proteolytic activity in Y153F casp-9. Second, it is important to note that Tyr-397 is contained within a much more ideal c-Abl recognition site than Tyr-153 is. Third, c-Abl phosphorylation of casp-9 at Tyr-153 was reported after induction of DNA damage (12). c-Abl is known to shuttle between the cytosol and the nucleus (34), and DNA damage activates nuclear c-Abl (35, 36). It is possible that c-Abl activated by DNA damage has an altered sequence specificity or recognizes casp-9 in complex with cofactors that direct phosphorylation to Tyr-153 or that it prefers to phosphorylate Tyr-153 in casp-9 in a different conformational state. We are only able to speculate on the altered specificity or complex formation, but we have evidence that the conformational state is not likely to contribute significantly to the ability of c-Abl to recognize casp-9. We found that neither casp-9 in the zymogen nor casp-9 in the cleaved state was phosphorylated at Tyr-153 (Figs. 2 (B and D) and 3 (C and D)) *in*

vitro. Fourth, cases of multisite phosphorylation on proteins resulting in antagonistic effects have been reported (37, 38), so it is possible that two sites in casp-9 are differentially phosphorylated by c-Abl *in vivo*, in which phosphorylation at Tyr-153 could lead to casp-9 activation, whereas phosphorylation at Tyr-397 results in casp-9 inhibition. Finally, and most probably, it is also possible that c-Abl activated by DNA damage activates another kinase that is responsible for Tyr-153 phosphorylation. The fact that Tyr-397 is contained within a more ideal c-Abl recognition site than Tyr-153 may also suggest that Tyr-153 phosphorylation is achieved not by c-Abl directly, but by a different kinase that is activated by c-Abl or by the same stimuli that activate c-Abl.

Tyr-397 is present in the L4 loop, which forms the side of the substrate-binding groove in caspases. This site is a privileged location for regulation in that it is adjacent to but does not directly interact with substrate. No phosphorylatable tyrosines are present in the L4 loops of other caspases (supplemental Fig. S7, A and B), so phosphorylation by c-Abl and inhibition by this active site-adjacent mechanism is likely to be unique to casp-9. Thus, Tyr-397 may provide a chemical handle for development of compounds that inhibit casp-9 specifically. Interestingly, in casp-6, Cys-264, which is also in the L4 loop, is palmitoylated (39). The functional impact of this palmitoylation has not been fully uncovered, but it is tempting to speculate that, like casp-9

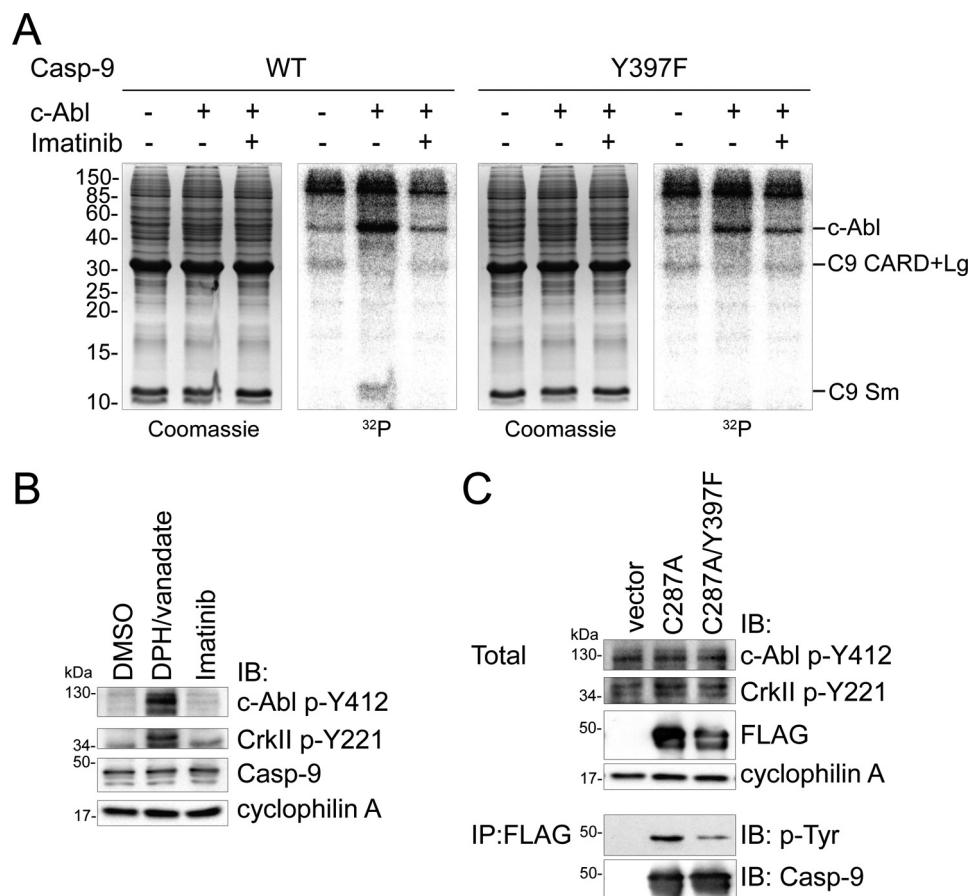


Figure 6. Activation of c-Abl leads to casp-9 phosphorylation at Tyr-397 intracellularly. *A*, recombinant casp-9 was phosphorylated in HEK 293T lysates. Lysates were supplemented with 20 nM c-Abl, 200 μ M orthovanadate, and 1 mM ATP + [γ -³²P]ATP to ensure *in trans* activation of c-Abl. Where indicated, lysates were also treated with the c-Abl inhibitor imatinib (200 μ M) 30 min before the addition of c-Abl. WT or Y397F casp-9 (30 μ g) were added to lysates to allow casp-9 phosphorylation. WT but not Y397F casp-9 showed phosphorylation in the small (Sm) subunit, which was not visible with imatinib-treated lysates. In some trials, the small subunit of Y397F also appears to be labeled, albeit at a significantly lower level than that of WT (supplemental Fig. S5, B and C). The phosphorylation observed for CARD+Large appeared to be c-Abl-independent, because imatinib did not eliminate its phosphorylation. *B*, c-Abl is activated by DPH in synergy with orthovanadate treatment. HEK 293T cells were treated with DMSO, the known c-Abl-activating compound DPH + orthovanadate, or imatinib for 2 h. Lysates were probed for active c-Abl as assessed by immunoblotting (IB). Active c-Abl is phosphorylated at Tyr-412. DPH/vanadate treatment clearly resulted in c-Abl activation, as manifested by phosphorylation at Tyr-412 and downstream phosphorylation of a well-known c-Abl substrate, CrkII, at Tyr-221. *C*, Casp-9 is phosphorylated at Tyr-397 by active c-Abl intracellularly. HEK 293T cells were transfected with vector alone (p3xFLAG-CMVTM-14), catalytic site-inactivated casp-9 (C9 C287A-3xFLAG), or the unphosphorylatable variant (C9 C287A/Y397F-3xFLAG). 24 h post-transfection, cells were treated with DPH/vanadate for 2 h, harvested, and lysed. Immunoblot of total proteins confirmed c-Abl activation and casp-9 expression. Casp-9 was immunoprecipitated from lysates with an anti-FLAG antibody and probed with anti-phosphotyrosine (p-Tyr) and anti-casp-9 by immunoblotting. Cells transfected with C287A/Y397F showed significantly lower levels of phosphotyrosine in uncleaved caspase-9 compared with those transfected with C287A, although the levels of immunoprecipitated casp-9 in both C287A and C287A/Y397F were similar.

Tyr-397 phosphorylation, casp-6 Cys-264 palmitoylation may result in loss of activity. The L4 has the most diverse sequence among the active-site loops in the apoptotic caspases; thus, posttranslational or targeted modification of L4 could be an amenable method of inhibition, as it might confer added specificity for each caspase.

Although the full impacts of Tyr-397 phosphorylation are not known, it is tempting to speculate about the functional impact of this phosphorylation event. A prevalent consequence of phosphorylation is its impact on protein-protein interactions. Phosphorylation can either disrupt or promote binding and in some cases even create a new binding interface. The region where Tyr-397 resides, ³⁹⁵GIYK³⁹⁸, in L4 of casp-9 is involved in crystal contacts (40), which may suggest that this region could potentially be involved in protein-protein binding under native conditions as well. Casp-9 is activated by recruitment to the apoptosome via CARD-

CARD interactions with Apaf-1 (41). Recently, a structure of the human apoptosome revealed that a monomer of casp-9 core (p20/p10) is "parked" on the apoptosome hub, probably in a dynamic manner, independent of the other casp-9 dimer(s) undergoing activation within the CARD-CARD ring (42). Monomeric casp-9 cores were also reported to bind to the apoptosome by forming a heterodimer with the Apaf-1 nucleotide oligomerization domain via the casp-9 small (p10) subunit (43). In addition, the apoptosome of *Caenorhabditis elegans* formed from CED4 and CED3 (homologues of Apaf-1 and casp-9, respectively) shows that the L2' region of Apaf-1 directly interacts with the oligomerized CED4 and is crucial in the formation of a functional holoenzyme (44). These observations imply that in addition to the CARD, other regions in casp-9 interact with the apoptosome and potentially influence its activation. Perhaps the Tyr-397 region of the small subunit is involved in direct interactions with the apoptosome,

Table 2
Molecular mechanisms of phosphorylation-mediated caspase inhibition

Molecular mechanism	Caspase	Site	Kinase ^a
Preventing zymogen activation	Casp-3	Tyr-174, Ser-176	CK2 (54)
	Casp-8	Tyr-380	Src (55, 56)
	Casp-9	Ser-310 (Ser-348 murine)	CK2 (10)
Blocking protein–protein interactions Disorienting substrate-binding loops	Casp-7	Ser-30	Pak2 (32)
	Casp-9	Ser-183	PKA (60)
	Casp-6	Ser-257	Ark5 (19)
Directly blocking substrate binding	Casp-7	Ser-239	Pak2 (32)
Core disruption and formation of ordered aggregates	Casp-9	Ser-183	PKA (60)
Active site-adjacent	Casp-9	Tyr-397	c-Abl

^aReferences in parentheses.

such that phosphorylation of Tyr-397 would impact these interactions.

c-Abl has been reported to play both proapoptotic and anti-apoptotic/prosurvival roles. The fact that casp-9 is inhibited by c-Abl phosphorylation at Tyr-397 suggests that this molecular event contributes to the prosurvival nature of c-Abl. Whereas c-Abl activation by DNA damage is known to induce cell death, hyperactive cytoplasmic kinase activities of c-Abl and Abl fusion proteins are recognized for their oncogenic potential (45, 46). A prime example is BCR-Abl fusion kinase, whose loss of autoinhibition and increased catalytic activity is highly persistent in chronic myelogenous leukemia (47, 48). Overexpression of c-Abl has been detected in certain breast tumors, colon and lung cancer carcinoma, and, in some cases, melanoma (46). c-Abl activation in most of these cases is thought to be either a result of deregulated activities of upstream kinases or activation of growth factor receptors, or both (26, 46). Besides deregulation and hyperactivity, the expanded diversity of Abl substrates due to altered specificities is thought to be another driving force toward oncogenicity (49, 50). Thus, c-Abl phosphorylation of pro-apoptotic proteins with a loss-of-function consequence is consistent with c-Abl's anti-apoptotic/prosurvival function. Targeting an initiator caspase, such as casp-9, serves as an efficient route to execute an upstream block in apoptosis signaling.

The dynamic cross-talk between caspases and kinases enables their co-regulation, which is essential for cellular homeostasis. In many cases, kinases are regulated by proteolysis by the very caspases they phosphorylate (6, 51). The cellular outcome, whether promotion or suppression of apoptosis, is dictated by which functional impact overcomes or precedes the other: caspase phosphorylation or kinase cleavage. We did not observe any apparent cleavage of c-Abl by casp-9 *in vitro*. One possibility is that casp-9 only exhibits basal or much lower levels of activity, whereas the kinase activity of c-Abl is heavily favored under *in vitro* phosphorylation conditions. It is also possible that c-Abl is simply not a preferred substrate of casp-9. However, the case might be different intracellularly because c-Abl was shown to be cleaved by casp-8 and casp-3, causing its transformation to an active state (52) and/or its relocation to the nucleus (53). Given that c-Abl exerts dual yet opposing functions in apoptosis, one could infer that the molecular dialogue between c-Abl and casp-9 would be more relevant in cell death signaling. We also observed that among apoptotic caspases, casp-9 is the most preferred substrate of c-Abl (supplemental Fig. S7C); we envision that exploiting this interaction could be a suitable approach to specifically control casp-9 function.

More phosphorylation sites have been reported in casp-9 than in any other caspase (for reviews, see Refs. 6–8). Perhaps this is simply due to the fact that more effort has focused on casp-9 or because there is a need for additional regulation of casp-9. The latter is more likely, as casp-9's upstream function requires exquisite control to prevent any inopportune amplification of apoptotic signals. Given the rapid rate of proteomics advancement, we expect more phosphorylation sites to be reported on caspases under different cellular conditions. In the study of the interactions of kinase with their substrates, it is often insufficient to rely solely on cell-based assays, particularly when the intrinsic activity of mutant enzymes has not been assessed. Accurately identifying functionally relevant sites and elucidating the mechanism of phosphoregulation requires complementary cellular, biochemical, and structural interrogation, as was done in this case.

Recent efforts by our group and others have begun to illuminate the diverse molecular mechanisms of phosphorylation-mediated caspase inhibition (Table 2). Some of these mechanisms operate by inhibiting the early stages of caspase activation, particularly zymogen activation. The conversion of caspases from a zymogen to a cleaved (mature) state to gain maximal activity is achieved by cleavage at the intersubunit linker, either by self-processing or by the action of another caspase. Phosphorylation of residues adjacent to or within the cleavage site(s) in the intersubunit linker has been shown to block linker cleavage, as observed in casp-3 (54), -8 (55, 56), and -9 (10). Recently, phosphorylation of casp-7 at a prodomain-adjacent Ser-30 was observed to block interaction with casp-9, leading to failure of casp-7 cleavage and activation (32). Phosphorylation also impacts the catalytic activity of mature caspases. The mobile nature of the active site loops allows the kinase facile access to phosphorylation sites that are in close proximity to or within the substrate-binding pocket. Phosphorylation of these residues appears to be a robust way to directly inhibit catalytic function either by blocking substrate binding through steric clash, as observed in casp-7 Ser-239 (32), or by disorienting the substrate-binding loops, thus making them incompetent to bind substrate, as in casp-6 Ser-257 and casp-9 Ser-183 (19, 60). We also observed an intriguing allosteric mechanism of phosphoregulation in casp-9 wherein phosphorylation of Ser-183 in the mature form is sufficient to disassemble the casp-9 core despite Ser-183 being distal from the large/small interface (60). Our recent data elucidating Tyr-397 phosphorylation adds to this list of caspase phosphoregulation. Our results clearly demonstrate that Tyr-397 in casp-9 is a *bona fide* site and the dominant site of phosphorylation by c-Abl

intracellularly. An active site-adjacent residue, Tyr-397, does not seem to participate in strong molecular interactions with residues within the substrate-binding pocket or with the substrate itself, but phosphorylation transforms this site to one that directly inhibits substrate binding. This is the first report of a novel c-Abl phosphorylation site unique to casp-9, and targeting Tyr-397 may serve as an alternative approach for the specific control of casp-9. Our results suggest that phosphorylation of casp-9 by c-Abl is an important mechanism by which c-Abl fulfills its survival role to escape apoptosis. The next studies prompted by these findings are to determine the level of casp-9 phosphorylation at Tyr-397 in cancer cells where c-Abl is over-expressed and hyperactive, as it may provide possible avenues for caspase-kinase co-therapies in cancer and other proliferative diseases.

Experimental procedures

DNA constructs

The casp-9 full-length wild-type (C9FL WT) expression construct (gift of Guy Salvesen) consists of the human casp-9 gene (amino acids 1–416) with C-terminal His₆ tag in pET23b (57). The casp-9 constitutively two-chain (CT) construct consists of an *Escherichia coli* codon-optimized synthetic gene (GenScript) built for expression of the CARD+Large subunit (amino acids 1–315) and separate expression of the small subunit (amino acids 316–416 plus His₆), which was under the control of a second ribosome-binding site. The casp-9 Δ CARD expression construct was made by deleting the CARD in the C9FL construct by deletion mutagenesis and inserting a start codon before the first amino acid (Val-139) of the large subunit. Casp-3 full-length wild-type expression construct (gift of Guy Salvesen) consists of the human casp-3 gene (amino acids 1–279 plus His₆) in pET23b (58). Caspase variants encoding amino acid substitutions were generated by point mutagenesis. Bacterial expression constructs for the c-Abl kinase domain (c-Abl kinase) (amino acids 229–511) in pET28a, c-Abl SH3-SH2-kinase domains (c-Abl 3D) (amino acids 46–515) in pET28a, and YopH phosphatase in pCDFDuet-1 were gifts from Markus Seeliger (59) (Stony Brook University School of Medicine). Both c-Abl constructs have a TEV protease-cleavable His₆ tag at the N termini.

For casp-9 expression in HEK 293T cells, casp-9 FL C287A or FL C287A/Y397F gene was subcloned between HindIII and BamHI sites of the p3xFLAG-CMVTM-14 vector (Sigma), producing a C-terminally 3xFLAG-tagged casp-9 expression construct.

Expression and purification of proteins

Purification of casp-9 proteins—Casp-9 (FL, CT, and Δ CARD expression constructs) in pET23b were individually transformed into the BL21(DE3) *E. coli* strain. Cells were grown in 2 \times YT medium with 100 μ g/ml ampicillin at 37 $^{\circ}$ C with shaking until $A_{600} = 1.2$. The temperature was lowered to 15 $^{\circ}$ C, and protein expression was induced with 1 mM IPTG for 3 h. Cells were harvested by centrifugation at 4,700 \times g for 10 min at 4 $^{\circ}$ C. Thawed cells were resuspended in a buffer containing 50 mM sodium phosphate, pH 7.0, 300 mM NaCl, 2 mM imidazole and lysed by use of a microfluidizer (Microfluidics, Inc.). Cell lysate

was clarified by centrifugation at 37,000 \times g for 1 h at 4 $^{\circ}$ C. The supernatant was then loaded onto a HiTrap nickel affinity column (GE Healthcare). Proteins were eluted using a linear imidazole gradient from 2 to 100 mM. Fractions containing casp-9 were pooled, diluted 8-fold in 20 mM Tris, pH 8.5, 5 mM DTT and loaded onto a HiTrap Q-column (GE Healthcare). Proteins were eluted using a linear NaCl gradient from 0 to 275 mM. Casp-9 eluted in buffer with 180 mM NaCl. Peak fractions were analyzed by SDS-PAGE for purity and stored in -80° C until further use.

Purification of casp-3—Full-length casp-3 (wild-type or the catalytic site-inactivated variant C163S expression constructs) in pET23b were individually transformed into the BL21(DE3) strain of *E. coli*. Cultures were grown in 2 \times YT medium supplemented with 100 μ g/ml ampicillin at 37 $^{\circ}$ C with shaking until $A_{600} = 0.8$. The temperature was lowered to 30 $^{\circ}$ C, and protein expression was induced by 1 mM IPTG for 3 h. Cells were harvested by centrifugation at 4,700 \times g for 10 min at 4 $^{\circ}$ C. Cells were freeze-thawed, resuspended in lysis buffer (50 mM sodium phosphate, pH 8, 300 mM NaCl, 2 mM imidazole), and lysed by use of a microfluidizer. Lysed cells were centrifuged at 37,000 \times g for 50 min at 4 $^{\circ}$ C to remove cellular debris. The supernatant was loaded onto a HiTrap nickel-affinity column. The column was then washed with 50 mM imidazole in lysis buffer, and proteins were eluted with 250 mM in lysis buffer. The eluent was diluted 6-fold with buffer A (20 mM Tris, pH 8.0, 3 mM DTT) and loaded onto a HiTrap Q-column. Proteins were eluted using a linear gradient from 0 to 500 mM NaCl. Casp-3 eluted in buffer A with 250 mM NaCl. Peak fractions were analyzed by SDS-PAGE for purity and stored in -80° C until use.

Purification of c-Abl kinase—c-Abl kinase was purified according to a method developed by Seeliger *et al.* (59). Briefly, the expression constructs for c-Abl in pET28a and for YopH in pCDFDuet were co-transformed in BL21(DE3) *E. coli* cells. Cells were grown in 2 \times YT medium supplemented with kanamycin (50 μ g/ml) and streptomycin (50 μ g/ml) at 37 $^{\circ}$ C with shaking until $A_{600} = 1.2$. The temperature was lowered to 18 $^{\circ}$ C, and protein expression was induced with 0.2 mM IPTG for 16 h. Cells were harvested by centrifugation at 4,700 \times g at 4 $^{\circ}$ C and stored at -80° C until use. Thawed cells were resuspended in lysis buffer (50 mM Tris, pH 8.0, 500 mM NaCl, 5% glycerol, 25 mM imidazole), lysed by passing through a microfluidizer, and centrifuged at 37,000 \times g for 1 h at 4 $^{\circ}$ C. The supernatant was loaded onto a 5-ml HiTrap nickel affinity column. Proteins were eluted using a linear gradient of 25–250 mM imidazole in lysis buffer. Fractions containing c-Abl were pooled and treated with TEV protease to cleave the His tag (1 mg of TEV per 25 mg of crude kinase). Cleavage proceeded at 4 $^{\circ}$ C for 16 h while dialyzing against 20 volumes of buffer A (20 mM Tris, pH 8.0, 100 mM NaCl, 5% glycerol, and 1 mM DTT). The dialysate was diluted 2-fold with buffer A and loaded onto a HiTrap Q column. The column was developed using a linear gradient of 100–350 mM NaCl in buffer A. c-Abl eluted in buffer A with 200 mM NaCl. Peak fractions were analyzed by SDS-PAGE for purity and stored at -80° C until use.

Caspase-9 phosphorylation by *c-Abl*

In vitro phosphorylation of casp-9

Autophosphorylation of *c-Abl*—*c-Abl* (20 μM) was incubated in kinase activity buffer (50 mM Tris-Cl, pH 7.5, 20 mM MgCl_2 , 0.1 mM EDTA, 0.5 mM EGTA, 5 mM β -glycerophosphate, 1 mM Na_3VO_4) and allowed to autoactivate in the presence of 250 μM ATP with [γ - ^{32}P]ATP (10 $\mu\text{Ci}/\mu\text{l}$; PerkinElmer Life Sciences) for 2 h at 30 °C.

Phosphorylation of casp-9—Casp-9 (50 μM) was incubated with 1 μM autoactivated *c-Abl* in kinase activity buffer with 1 mM ATP containing [γ - ^{32}P]ATP for 4 h at 30 °C. For phosphorylation of casp-9 in HEK 293T lysates, 20 nM *c-Abl* was incubated first with the lysates (150 μg of total protein) with or without imatinib (200 μM ; Sigma) for 30 min. Casp-9, WT, or Y397F (30 μg) was then added, and the reaction was allowed to proceed for 4 h at 30 °C.

Phosphoenrichment—*c-Abl*-phosphorylated casp-9 WT (100 μM) was buffer-exchanged into a loading buffer (TALON[®] PMAC kit, Clontech) using a NAP[™]5 desalting column (GE Healthcare). The buffer-exchanged protein solution was then mixed with TALON[®] PMAC magnetic beads (Clontech) for 1 h at 4 °C. The beads were washed twice with loading buffer, and phosphorylated proteins were eluted from the beads using 250 mM sodium phosphate, pH 7.2, 0.5 M NaCl. Protein concentrations of eluted fractions were estimated using a BCA assay kit (Pierce[™], Thermo Scientific).

All reactions were stopped by the addition of SDS-PAGE sample dye and boiling for 10 min. Proteins were resolved by denaturing SDS-PAGE. Phosphor images were obtained using Typhoon FLA 7000 (GE Healthcare), and bands were quantified using ImageQuant TL software (GE Healthcare). The amount of phosphate incorporated was quantified from an ATP standard curve on the same phosphor image (supplemental Fig. S2).

Casp-9 activity assay

Casp-9 was diluted in casp-9 activity assay buffer (100 mM MES, pH 6.5, 10% PEG 8000, 5 mM DTT) to a final concentration of 800 nM. For determination of catalytic parameters, a substrate titration was performed in the range of 0–3 mM fluorogenic substrate *N*-acetyl-Leu-Glu-His-Asp-7-aminotrifluoromethylcoumarin (excitation 365 nm/emission 495 nm) (Enzo Life Sciences). A non-linear fit was used to estimate K_m using Prism software (GraphPad Software, Inc.) Enzyme concentrations were determined by active-site titration using a quantitative inhibitor, benzoyloxycarbonyl-Val-Ala-Asp-[*O*-methyl]fluoromethylketone (Enzo Life Sciences). The rate of LEHD cleavage (LEHDase) was measured using a Spectramax M5 fluorescence plate reader (Molecular Devices). For casp-9 activity assays after phosphorylation, 1.5 μM casp-9 and 1 mM substrate were used.

Cleavage assays

Self-cleavage—Zymogen forms of casp-9 (WT, Y153E, Y153D, and Y153F) (3 μM) were allowed to undergo self-cleavage in a minimal activity assay buffer (100 mM MES, pH 6.5, 20% PEG 400, 5 mM DTT) at 37 °C over the course of 2 h.

Cleavage by casp-3—Casp-3 WT (20 nM) was prepared in casp-3 activity assay buffer (20 mM HEPES, pH 7.5, 150 mM

NaCl, 5 mM CaCl_2 , 10% PEG 400, 2 mM DTT). Full-length, uncleaved casp-9 (catalytic site-inactivated variant C287A, phosphomimetics Y153E and Y153D, or Y153F) (5 μM) was added, and the reaction was incubated at 37 °C for the times indicated.

Cleavage of casp-3 and casp-7 by casp-9—Casp-9 WT or Y397F (50 μM) was initially phosphorylated by *c-Abl*. Phosphorylated (WT) and unphosphorylated (Y397F) casp-9 was then diluted to 1 μM in casp-9 minimal activity buffer, after which each of the catalytic site-inactivated variants of casp-3 C163S or casp-7 C186A were added to a final concentration of 3 μM and incubated at 32 °C. Aliquots were taken at different time points within 30 min.

All cleavage reactions were stopped by the addition of SDS-PAGE sample buffer and boiling for 10 min. Bands were quantified by densitometry using ImageLab software (Bio-Rad).

Cell culture, transfections, and preparation of extracts—HEK 293T cells were grown in RPMI medium supplemented with 10% fetal bovine serum, 2 mM glutamine, 50 IU of penicillin, 50 $\mu\text{g}/\text{ml}$ streptomycin, and 2 mM sodium pyruvate. Cells were incubated at 37 °C in a humidified atmosphere maintained at 5% CO_2 . Cells were transiently transfected with either empty vector (p3xFLAG-CMV-14) or casp-9 (C9 C287A-3xFLAG or C9 C287A/Y397F-3xFLAG), using the X-tremeGENE HP DNA transfection reagent (Roche Applied Science) according to the manufacturer's instructions.

After 24 h of expression, transfected cells were washed with 1 \times PBS and lysed with 1 \times modified Barth's saline–Triton X-100, pH 7.8, containing 5 mM HEPES, pH 7.8, 176 mM NaCl, 1 mM KCl, 1 mM MgSO_4 , 2.5 mM NaHCO_3 , 1% Triton X-100, and supplemented with Halt[™] protease and phosphatase inhibitor mixture (Thermo Scientific). Lysates were clarified by centrifugation for 30 min at 16,100 $\times g$ at 4 °C.

Activation of *c-Abl* in HEK 293T

Transfected HEK 293T cultures grown to ~90% confluence were treated with 20 μM 5-(1,3-diaryl-1H-pyrazol-4-yl)hydantoin (DPH) (Sigma) and 100 μM sodium orthovanadate (Sigma) for 2 h. For untreated cells, DMSO was added in place of DPH. To determine the inhibition of endogenous *c-Abl*, HEK 293T cells were initially treated with 20 μM imatinib mesylate (Sigma) for 16 h before DPH treatment. Activation was assessed by monitoring autophosphorylation of *c-Abl* at Tyr-412 and phosphorylation of known *c-Abl* substrate CrkII by immunoblot.

Immunoprecipitation and immunoblotting

3xFLAG-tagged casp-9 from lysates of transfected cells were immunoprecipitated using anti-FLAG[®] M2 affinity gel (Sigma). The beads with covalently linked antibody were incubated with the lysates for 16 h at 4 °C using an end-to-end rotator. Beads were washed three times with 1 \times modified Barth's saline–Triton X-100 buffer with Halt[™] protease and phosphatase inhibitor mixture (Thermo Scientific). Immunoprecipitates were eluted with non-denaturing Laemmli buffer, after which 5 mM DTT (final concentration) was added, and the solution was boiled for 5 min. Total lysates and immunoprecipitates were loaded onto a 5–22% SDS-polyacrylamide gel and electroblotted to a PVDF membrane. Total lysates were probed with

antibodies against the following: FLAG (mouse, clone M2; Millipore), pTyr-412 c-Abl (rabbit; Cell Signaling Technologies), pTyr-221 CrkII (rabbit; Cell Signaling Technologies), casp-9 (rabbit; Cell Signaling Technologies), and cyclophilin A (rabbit; Cell Signaling Technologies), which served as a loading control. Antibody-antigen complexes were probed with anti-phosphotyrosine (mouse, 4G10 Platinum; Millipore) and anti-casp-9 (mouse; Proteintech). All primary antibodies were used at 1:1000 dilution. Before immunoblotting with anti-casp-9, the membrane was stripped using a stripping buffer, pH 2.2 (20 mM glycine, 0.1% (w/v) SDS, 1% Tween) for 1 h and then washed sequentially with 1× PBS and 1× TBST. Stripping was confirmed by probing with a secondary antibody and visualizing no bands after substrate incubation. The following HRP-conjugated secondary antibodies were used (all from Jackson ImmunoResearch): goat anti-mouse IgG, goat anti-mouse IgG light chain-specific, goat anti-rabbit IgG. Immunoreactive bands were detected by enhanced chemiluminescence using an X-ray film and by visualizing in ChemiDoc XRS+ (Bio-Rad). For detection by X-ray film, secondary antibodies were diluted 1:5000; for detection by ChemiDoc XRS+, secondary antibodies were diluted 1:50,000.

Protein digestion and LC-MS/MS

In-solution digestion—Casp-9 (50 μM) was phosphorylated by c-Abl (1 μM) with 1 mM ATP for 4 h at 30 °C. After phosphorylation, 5 mM DTT (final concentration) was added and incubated at 30 °C for 20 min. Cysteine alkylation was then performed by treatment of the sample with 8 mM iodoacetamide (Sigma). The tube was covered with foil to prevent light-mediated reactions, and the reaction was agitated using an end-to-end rotator for 15 min at room temperature. Unreacted iodoacetamide was quenched by adding 5 mM DTT for 15 min at room temperature. Half of this reaction (~ 100 μg of casp-9) was diluted in the same volume of Arg-C incubation buffer (50 mM Tris, pH 7.7, 5 mM CaCl_2 , and 2 mM EDTA). 1 μg of Arg-C protease (sequencing grade; Promega) in 50 μl of activation buffer (5 mM Tris-Cl, pH 7.7, 5 mM DTT, 200 μM EDTA) was then added to the reaction. Digestion was allowed to proceed for 16 h at 37 °C. The reaction was stopped by adding 10% formic acid to a final concentration of 0.5%. Final pH was confirmed to be ≤ 2.0 . Arg-C was removed using a Microcon[®] spin filter column, molecular weight cut-off 10,000 (Millipore), centrifuged at $16,100 \times g$ for 15 min. Peptide concentration was estimated by absorbance at 280 nm using a NanoDrop[™] 2000c spectrophotometer (Thermo Scientific). Digested proteins were diluted with 1% formic acid to contain 2 μg of peptides.

LC-MS/MS—Protein digests were diluted in 0.1% formic acid in water (solvent A) and were analyzed on an Orbitrap Fusion[™] mass spectrometer (Thermo Scientific) coupled to an Easy-nLC 1000 (Thermo Scientific) ultra-HPLC pump. Analytical LC separations were performed on a FortisBIO C18 nano-flow column (150 mm \times 75 μm , 1.7 μm (Fortis Technologies Ltd.)) at a flow rate of 225 nl/min. The following step gradient was used: 0–40% solvent B (0.1% formic acid in acetonitrile) for the first 90 min and then 40–85% B for 90–95 min. Total run time was set to 130 min. MS1 spectra were collected on a positive polarity mode with a scan range from m/z

350 to 1,500 at a resolution of 120,000 with an automated gain control target of 400,000 and a maximum injection time of 50 ms. The most intense ions were selected for MS/MS. A dynamic exclusion window of 60 s with a mass tolerance of ± 10 ppm was used to exclude precursors. MS2 precursors were isolated with a quadrupole mass filter, fragmented by electron transfer dissociation, and detected by an ion trap mass analyzer. MS2 was operated with an automated gain control target of 50,000 and a maximum injection time of 100 ms. MS/MS analysis workflow was created with Proteome Discoverer version 1.4 (Thermo Scientific). Assignment of MS/MS spectra was performed using the SEQUEST algorithm utilizing the FASTA sequence for human casp-9 (UniProt ID P55211). SEQUEST searches were performed with a 10-ppm precursor mass tolerance and 0.5-Da fragment mass tolerance while requiring peptide termini to have Arg-C protease specificity and allowing up to three missed cleavages. Carbamidomethylation of cysteine residues (+57.021 Da) and phosphorylation of tyrosine residues (+79.966) were set as dynamic modifications.

Author contributions—B. P. S. designed, initiated, and performed all experiments and data analysis and prepared all figures and is the principal author of the manuscript. H. S. S. performed some of the cell culture experiments. D. R. A. designed cell culture experiments and edited the manuscript. J. A. H. conceptualized and directed the research project, secured funding, analyzed and interpreted data, and wrote and edited parts of the manuscript. All authors reviewed the manuscript and approved of its submission in the final form.

Acknowledgment—We thank Stephen Eyles, Director of the UMass Mass Spectrometry facility, for assistance with mass spectrometric analysis.

References

- Alnemri, E. S., Livingston, D. J., Nicholson, D. W., Salvesen, G., Thornberry, N. A., Wong, W. W., and Yuan, J. (1996) Human ICE/CED-3 protease nomenclature. *Cell* **87**, 171
- Checińska, A., Giaccone, G., Rodriguez, J. A., Krzyt, F. A. E., and Jimenez, C. R. (2009) Comparative proteomics analysis of caspase-9-protein complexes in untreated and cytochrome *c*/dATP stimulated lysates of NSCLC cells. *J Proteomics* **72**, 575–585
- Seaman, J. E., Julien, O., Lee, P. S., Rettenmaier, T. J., Thomsen, N. D., and Wells, J. A. (2016) Caspases: caspases can cleave after aspartate, glutamate and phosphoserine residues. *Cell Death Differ.* **23**, 1717–1726
- Franklin, R. A., and McCubrey, J. A. (2000) Kinases: positive and negative regulators of apoptosis. *Leukemia* **14**, 2019–2034
- López-Otín, C., and Hunter, T. (2010) The regulatory crosstalk between kinases and proteases in cancer. *Nat. Rev. Cancer* **10**, 278–292
- Kurokawa, M., and Kornbluth, S. (2009) Caspases and kinases in a death grip. *Cell* **138**, 838–854
- Dagbay, K., Eron, S. J., Serrano, B. P., Velázquez-Delgado, E. M., Zhao, Y., Lin, D., Vaidya, S., and Hardy, J. A. (2014) A multipronged approach for compiling a global map of allosteric regulation in the apoptotic caspases. *Methods Enzymol.* **544**, 215–249
- Zamaraev, A. V., Kopeina, G. S., Prokhorova, E. A., Zhivotovsky, B., and Lavrik, I. N. (2017) Post-translational modification of caspases: the other side of apoptosis regulation. *Trends Cell Biol.* **27**, 322–339
- Allan, L. A., and Clarke, P. R. (2007) Phosphorylation of caspase-9 by CDK1/cyclin B1 protects mitotic cells against apoptosis. *Mol. Cell* **26**, 301–310
- McDonnell, M. A., Abedin, M. J., Melendez, M., Platikanova, T. N., Ecklund, J. R., Ahmed, K., and Kelekar, A. (2008) Phosphorylation of murine

Caspase-9 phosphorylation by c-Abl

- caspase-9 by the protein kinase casein kinase 2 regulates its cleavage by caspase-8. *J. Biol. Chem.* **283**, 20149–20158
11. Brady, S. C., Allan, L. A., and Clarke, P. R. (2005) Regulation of caspase 9 through phosphorylation by protein kinase C ζ in response to hyperosmotic stress. *Mol. Cell. Biol.* **25**, 10543–10555
 12. Raina, D., Pandey, P., Ahmad, R., Bharti, A., Ren, J., Kharbanda, S., Weichselbaum, R., and Kufe, D. (2005) c-Abl tyrosine kinase regulates caspase-9 autocleavage in the apoptotic response to DNA damage. *J. Biol. Chem.* **280**, 11147–11151
 13. Cardone, M. H., et al. (1998) Regulation of cell death protease caspase-9 by phosphorylation. *Science* **282**, 1318–1321
 14. Allan, L. A., Morrice, N., Brady, S., Magee, G., Pathak, S., and Clarke, P. R. (2003) Inhibition of caspase-9 through phosphorylation at Thr 125 by ERK MAPK. *Nat. Cell Biol.* **5**, 647–654
 15. Seifert, A., Allan, L. A., and Clarke, P. R. (2008) DYRK1A phosphorylates caspase 9 at an inhibitory site and is potently inhibited in human cells by harmine. *FEBS J.* **275**, 6268–6280
 16. Allan, L. A., and Clarke, P. R. (2009) Apoptosis and autophagy: regulation of caspase-9 by phosphorylation. *FEBS J.* **276**, 6063–6073
 17. Wang, J. Y. J. (2014) The capable ABL: what is its biological function? *Mol. Cell. Biol.* **34**, 1188–1197
 18. Witkowski, W. A., and Hardy, J. A. (2009) L2' loop is critical for caspase-7 active site formation. *Protein Sci.* **18**, 1459–1468
 19. Velázquez-Delgado, E. M., and Hardy, J. A. (2012) Phosphorylation regulates assembly of the caspase-6 substrate-binding groove. *Structure* **20**, 742–751
 20. Slee, E. A., Harte, M. T., Kluck, R. M., Wolf, B. B., Casiano, C. A., Newmeyer, D. D., Wang, H. G., Reed, J. C., Nicholson, D. W., Alnemri, E. S., Green, D. R., and Martin, S. J. (1999) Ordering the cytochrome *c*-initiated caspase cascade: hierarchical activation of caspases-2, -3, -6, -7, -8 and -10 in a caspase-9-dependent manner. *J. Cell Biol.* **144**, 281–292
 21. Manning, B. D., and Cantley, L. C. (2002) Hitting the target: emerging technologies in the search for kinase substrates. *Sci. STKE* **2002**, pe49
 22. Martin, M. C., Allan, L. A., Lickrish, M., Sampson, C., Morrice, N., and Clarke, P. R. (2005) Protein kinase A regulates caspase-9 activation by Apaf-1 downstream of cytochrome *c*. *J. Biol. Chem.* **280**, 15449–15455
 23. Laguna, A., Aranda, S., Barallobre, M. J., Barhoum, R., Fernández, E., Fotaki, V., Delabar, J. M., de la Luna, S., de la Villa, P., Arbonés, M. L. (2008) The protein kinase DYRK1A regulates caspase-9-mediated apoptosis during retina development. *Dev. Cell* **15**, 841–853
 24. Pendergast, A. M. (2002) The Abl family kinases: mechanisms of regulation and signaling. *Adv. Cancer Res.* **85**, 51–100
 25. Srinivasan, D., and Plattner, R. (2006) Activation of Abl tyrosine kinases promotes invasion of aggressive breast cancer cells. *Cancer Res.* **66**, 5648–5655
 26. Plattner, R., Kadlec, L., DeMali, K. A., Kazlauskas, A., and Pendergast, A. M. (1999) c-Abl is activated by growth factors and Src family kinases and has a role in the cellular response to PDGF. *Genes Dev.* **13**, 2400–2411
 27. Yang, J., Campobasso, N., Biju, M. P., Fisher, K., Pan, X. Q., Cottom, J., Galbraith, S., Ho, T., Zhang, H., Hong, X., Ward, P., Hofmann, G., Siegfried, B., Zappacosta, F., Washio, Y., et al. (2011) Discovery and characterization of a cell-permeable, small-molecule c-Abl kinase activator that binds to the myristoyl binding site. *Chem. Biol.* **18**, 177–186
 28. Brasher, B. B., and Van Etten, R. A. (2000) c-Abl has high intrinsic tyrosine kinase activity that is stimulated by mutation of the Src homology 3 domain and by autophosphorylation at two distinct regulatory tyrosines. *J. Biol. Chem.* **275**, 35631–35637
 29. Feller, S. M., Knudsen, B., and Hanafusa, H. (1994) c-Abl kinase regulates the protein binding activity of c-Crk. *EMBO J.* **13**, 2341–2351
 30. Cheng, H.-C., Matsuura, I., and Wang, J. H. (1993) *In vitro* substrate specificity of protein tyrosine kinases. In *Reversible Protein Phosphorylation in Cell Regulation*, pp. 103–112, Springer, Boston, MA
 31. Johnson, S. A., and Hunter, T. (2005) Kinomics: methods for deciphering the kinome. *Nat. Methods* **2**, 17–25
 32. Eron, S. J., Raghupathi, K., and Hardy, J. A. (2017) Dual site phosphorylation of caspase-7 by PAK2 blocks apoptotic activity by two distinct mechanisms. *Structure* **25**, 27–39
 33. Hornbeck, P. V., Zhang, B., Murray, B., Kornhauser, J. M., Latham, V., and Skrzypek, E. (2015) PhosphoSitePlus, 2014: mutations, PTMs and recalibrations. *Nucleic Acids Res.* **43**, D512–D520
 34. Taagepera, S., McDonald, D., Loeb, J. E., Whitaker, L. L., McElroy, A. K., Wang, J. Y., and Hope, T. J. (1998) Nuclear-cytoplasmic shuttling of C-ABL tyrosine kinase. *Proc. Natl. Acad. Sci. U.S.A.* **95**, 7457–7462
 35. Kharbanda, S., Ren, R., Pandey, P., Shafman, T. D., Feller, S. M., Weichselbaum, R. R., and Kufe, D. W. (1995) Activation of the c-Abl tyrosine kinase in the stress response to DNA-damaging agents. *Nature* **376**, 785–788
 36. Shaul Y. (2000) c-Abl: activation and nuclear targets. *Cell Death Differ.* **7**, 10–16
 37. Mylona, A., Theillet, F. X., Foster, C., Cheng, T. M., Miralles, F., Bates, P. A., Selenko, P., and Treisman, R. (2016) Opposing effects of Elk-1 multisite phosphorylation shape its response to ERK activation. *Science* **354**, 233–237
 38. Vanselow, K., Vanselow, J. T., Westermarck, P. O., Reischl, S., Maier, B., Korte, T., Herrmann, A., Herzog, H., Schlosser, A., and Kramer, A. (2006) Differential effects of PER2 phosphorylation: molecular basis for the human familial advanced sleep phase syndrome (FASPS). *Genes Dev.* **20**, 2660–2672
 39. Skotte, N. H., Sanders, S. S., Singaraja, R. R., Ehrnhoefer, D. E., Vaid, K., Qiu, X., Kannan, S., Verma, C., and Hayden, M. R. (2017) Palmitoylation of caspase-6 by HIP14 regulates its activation. *Cell Death Differ.* **24**, 433–444
 40. Renatus, M., Stennicke, H. R., Scott, F. L., Liddington, R. C., and Salvesen, G. S. (2001) Dimer formation drives the activation of the cell death protease caspase-9. *Proc. Natl. Acad. Sci. U.S.A.* **98**, 14250–14255
 41. Qin, H., Srinivasula, S. M., Wu, G., Fernandes-Alnemri, T., Alnemri, E. S., and Shi, Y. (1999) Structural basis of procaspase-9 recruitment by the apoptotic protease-activating factor 1. *Nature* **399**, 549–557
 42. Cheng, T. C., Hong, C., Akey, I. V., Yuan, S., and Akey, C. W. (2016) A near atomic structure of the active human apoptosome. *Life* **5**, e17755
 43. Wu, C.-C., Lee, S., Malladi, S., Chen, M. D., Mastrandrea, N. J., Zhang, Z., and Bratton, S. B. (2016) The Apaf-1 apoptosome induces formation of caspase-9 homo- and heterodimers with distinct activities. *Nat. Commun.* **7**, 13565
 44. Huang, W., Jiang, T., Choi, W., Qi, S., Pang, Y., Hu, Q., Xu, Y., Gong, X., Jeffrey, P. D., Wang, J., and Shi, Y. (2013) Mechanistic insights into CED-4-mediated activation of CED-3. *Genes Dev.* **27**, 2039–2048
 45. Sirvent, A., Benistant, C., and Roche, S. (2008) Cytoplasmic signalling by the c-Abl tyrosine kinase in normal and cancer cells. *Biol. Cell* **100**, 617–631
 46. Greuber, E. K., Smith-Pearson, P., Wang, J., and Pendergast, A. M. (2013) Role of ABL family kinases in cancer: from leukaemia to solid tumours. *Nat. Rev. Cancer* **13**, 559–571
 47. Wong, S., and Witte, O. N. (2004) The BCR-ABL story: bench to bedside and back. *Annu. Rev. Immunol.* **22**, 247–306
 48. Hantschel, O., and Superti-Furga, G. (2004) Regulation of the c-Abl and Bcr-Abl tyrosine kinases. *Nat. Rev. Mol. Cell Biol.* **5**, 33–44
 49. Wu, J. J., Phan, H., and Lam, K. S. (1998) Comparison of the intrinsic kinase activity and substrate specificity of c-Abl and Bcr-Abl. *Bioorg. Med. Chem. Lett.* **8**, 2279–2284
 50. Voss, J., Posern, G., Hannemann, J. R., Wiedemann, L. M., Turhan, A. G., Poirel, H., Bernard, O. A., Adermann, K., Kardinal, C., and Feller, S. M. (2000) The leukaemic oncoproteins Bcr-Abl and Tel-Abl (ETV6/Abl) have altered substrate preferences and activate similar intracellular signalling pathways. *Oncogene* **19**, 1684–1690
 51. Dix, M. M., Simon, G. M., Wang, C., Okerberg, E., Patricelli, M. P., and Cravatt, B. F. (2012) Functional interplay between caspase cleavage and phosphorylation sculpts the apoptotic proteome. *Cell* **150**, 426–440
 52. Machuy, N., Rajalingam, K., and Rudel, T. (2004) Requirement of caspase-mediated cleavage of c-Abl during stress-induced apoptosis. *Cell Death Differ.* **11**, 290–300
 53. Barilà, D., Rufini, A., Condò, I., Ventura, N., Dorey, K., Superti-Furga, G., and Testi, R. (2003) Caspase-dependent cleavage of c-Abl contributes to apoptosis. *Mol. Cell. Biol.* **23**, 2790–2799

54. Duncan, J. S., Turowec, J. P., Duncan, K. E., Vilk, G., Wu, C., Lüscher, B., Li, S. S., Gloor, G. B., Litchfield, D. W. (2011) A peptide-based target screen implicates the protein kinase CK2 in the global regulation of caspase signaling. *Sci. Signal.* **4**, ra30
55. Tsang, J. L., Jia, S. H., Parodo, J., Plant, P., Lodyga, M., Charbonney, E., Szaszi, K., Kapus, A., and Marshall, J. C. (2016) Tyrosine phosphorylation of caspase-8 abrogates its apoptotic activity and promotes activation of c-Src. *PLoS One* **11**, e0153946
56. Powley, I. R., Hughes, M. A., Cain, K., and MacFarlane, M. (2016) Caspase-8 tyrosine-380 phosphorylation inhibits CD95 DISC function by preventing procaspase-8 maturation and cycling within the complex. *Oncogene* **35**, 5629–5640
57. Stennicke, H. R., Deveraux, Q. L., Humke, E. W., Reed, J. C., Dixit, V. M., and Salvesen, G. S. (1999) Caspase-9 can be activated without proteolytic processing. *J. Biol. Chem.* **274**, 8359–8362
58. Zhou, Q., Snipas, S., Orth, K., Muzio, M., Dixit, V. M., and Salvesen, G. S. (1997) Target protease specificity of the viral serpin CrmA: analysis of five caspases. *J. Biol. Chem.* **272**, 7797–7800
59. Seeliger, M. A., Young, M., Henderson, M. N., Pellicena, P., King, D. S., Falick, A. M., and Kuriyan, J. (2005) High yield bacterial expression of active c-Abl and c-Src tyrosine kinases. *Protein Sci.* **14**, 3135–3139
60. Serrano, B. P., and Hardy, J. A. (2017) Phosphorylation by protein kinase A disassembles the caspase-9 core. *Cell Death Differ.*, in press

Active site–adjacent phosphorylation at Tyr-397 by c-Abl kinase inactivates caspase-9

Banyuhay P. Serrano, Hannah S. Szydlo, Dominique Alfandari and Jeanne A. Hardy

J. Biol. Chem. 2017, 292:21352-21365.

doi: 10.1074/jbc.M117.811976 originally published online October 24, 2017

Access the most updated version of this article at doi: [10.1074/jbc.M117.811976](https://doi.org/10.1074/jbc.M117.811976)

Alerts:

- [When this article is cited](#)
- [When a correction for this article is posted](#)

[Click here](#) to choose from all of JBC's e-mail alerts

Supplemental material:

<http://www.jbc.org/content/suppl/2017/10/24/M117.811976.DC1>

This article cites 58 references, 20 of which can be accessed free at

<http://www.jbc.org/content/292/52/21352.full.html#ref-list-1>